We are IntechOpen, the world's leading publisher of Open Access books
Built by scientists, for scientists

4,800
Open access books available

122,000
International authors and editors

135M
Downloads

154
Countries delivered to

Our authors are among the

TOP 1%
most cited scientists

12.2%
Contributors from top 500 universities

BOOK CITATION INDEX
CLARIVATE ANALYTICS
INDEXED

WEB OF SCIENCE™

Selection of our books indexed in the Book Citation Index
in Web of Science™ Core Collection (BKCI)

Interested in publishing with us?
Contact book.department@intechopen.com

Chapter

Structural Evaluation of Bamboo Bike Frames: Experimental and Numerical Analysis

*Juan P. Arango Fierro, Jose L. Arango Fierro
and Héctor E. Jaramillo Suárez*

Abstract

Construction of bicycles with bamboo frames has become an alternative to improve the quality of life of some communities, be friendly with the environment and be ecologically sustainable. However, the production of bike frames is made in an artisanal way and there are few antecedents that have proven their reliability. This work presents the evaluation and simulation of the mechanical behavior of bike frames made in bamboo. Three-points bending tests were performed using bamboo bars with similar dimensions to bike frames, and an equivalent elasticity modulus was determined and used as the input datum of a finite element model. A linear model material and beam elements were used to model the bike frame. Tests were performed using bike frames of bamboo applying loads greater than 7000 N, and the displacements were measured. The experimental displacements were used to calibrate the model, which consisted of modifying the rigidity of the connections until the displacements of the model fit near to 90%. The calibrated model was used for a fatigue simulation in order to predict the lifespan of the bike frame. Some technical values of bamboo bike frames were obtained so that these will allow them to define the technical characteristics of the product and guarantee their operating conditions.

Keywords: bicycle, bike frame, bamboo, fatigue, three-point bending tests, finite element analysis

1. Introduction

Bicycles offer a cost-effective transportation alternative primarily for low-income communities [1]. Additionally, bikes have other advantages, such as zero greenhouse gas emissions, low-cost maintenance, quick displacement in high traffic zones, and physical fitness promotion for the users.

Conventional bike frames, using materials, such as steel [2], aluminum [2, 3], carbon fiber [4, 5], and titanium, have been studied via numerical model analyses and experimental tests. The numerical studies generally use the finite element method, and the tests generally obtain the static load carrying capacity; in this direction, the researches' focus has been oriented to improving the relationship between the weight and the strength. However, the new research trends are focused on the replacement of the bike frame material using a low-cost alternative, like

environmentally friendly materials, low weight and very attractive esthetically [6]. In this direction, the bamboo can become a good alternative.

There are more than 1000 species of bamboo around the world of which 70 are abundant in South America and Asia [7]. Bamboo is a natural fiber species that belongs to grass Poaceae family and subfamily Bambusoideae and grows in diverse types of climate. Compared to other trees, the bamboo has significant low density, high strength, and stiffness [8], most high growth rate (30–100 cm per day). Also, the bamboo plays an important environmental role by preventing ground erosion and landslides in mountainous zones and retaining significant amounts of water that restore ground conditions where it grows [9].

Currently, some companies and foundations have been building a bike frame using bamboo [10–12]. Locally, the bike frames are being manufactured using bamboo and their joints with a composite that uses an epoxy matrix reinforced with natural fibers (fique). However, the composite material joints are highly dependent on the geometric and material characteristics; for this reason, the testing of the actual bamboo bike frame is imperative. Some information can be found in the literature about the experimental strength of bamboo bike frame, although some analyses have been made using the finite element method [2, 13–15]. Once experimental data has been obtained, sensitivity and fatigue studies can be performed in order for the useful life of the bamboo bikes to be assessed.

In this direction, this work pretends to estimate the maximum allowable distance traveled by bikes made using bamboo frames. The general structural performance of the bike frames was evaluated under static and dynamic loads using experimental tests and the finite element method. Also, the mechanical strength of the joints was evaluated.

2. Methods and materials

Several steps were defined in order to perform the research (**Figure 1**). The first step was to determine the experimental properties of bamboo using a three-point bending test, measuring the displacement of some points of the bike under to external load and experimental modal analysis. The next step was to perform a static analysis of the bamboo bike frame using the finite element method. Using the experimental displacements, the finite element model was calibrated (step 3). The model calibrated was validated using the natural frequencies obtained experimentally (step 4). Finally, a fatigue analysis using the finite element method was performed using S-N curves reported and an estimation of the maximum distance that the bike can travel under the load conditions defined.

2.1 Geometry

The bamboo bike frames were made of bamboo tubes joined with a composite material, a resin as a matrix reinforced with fique (**Figure 2**).

A bamboo frame size M was used to perform the experiments and finite element analysis (**Figure 3**).

2.2 Experimental tests

#### 2.2.1 Three-point bending tests

Three-point bending tests were performed in order to characterize the structural behavior of bamboo. The load was applied perpendicularly at midspan of a simply
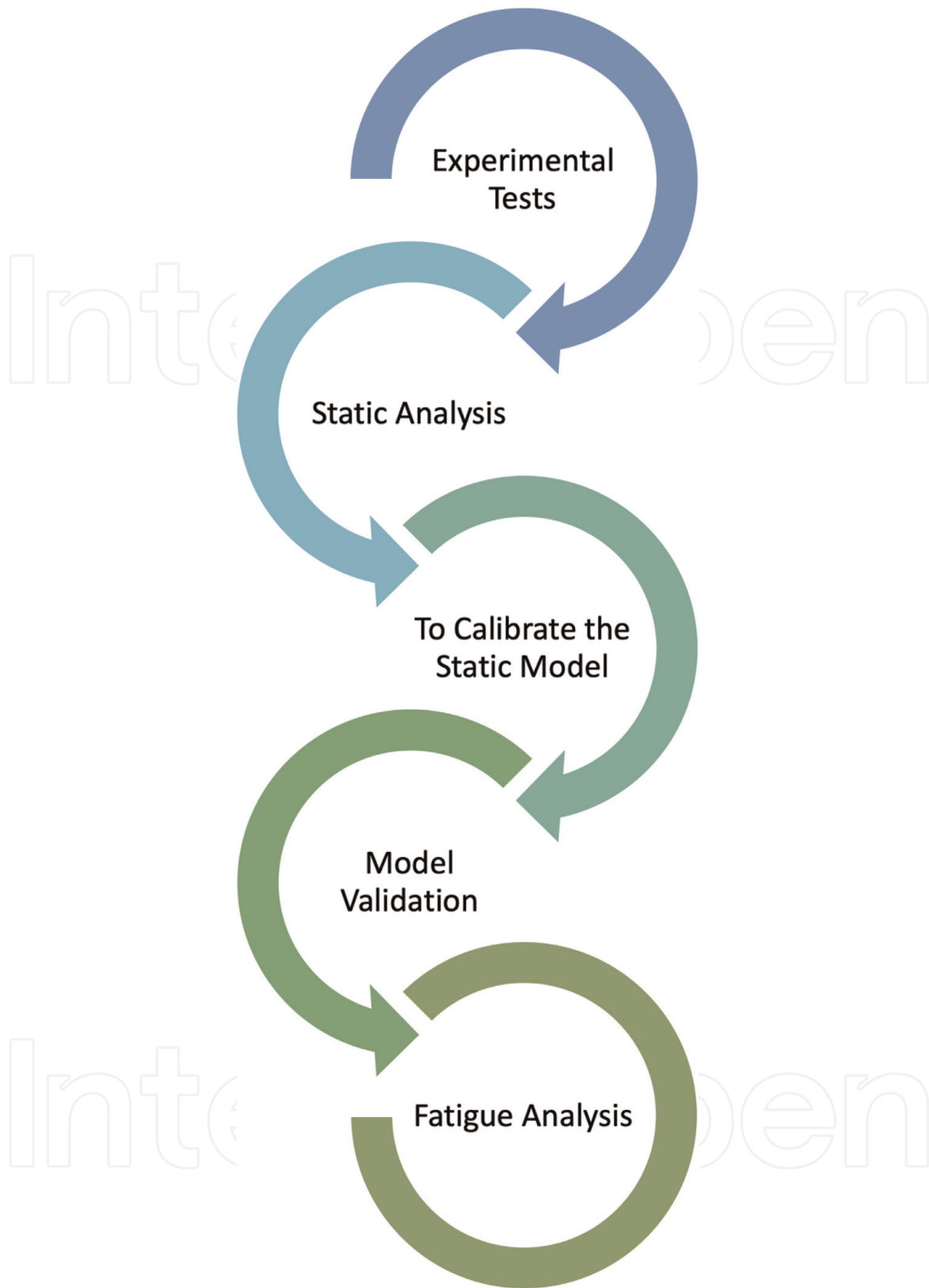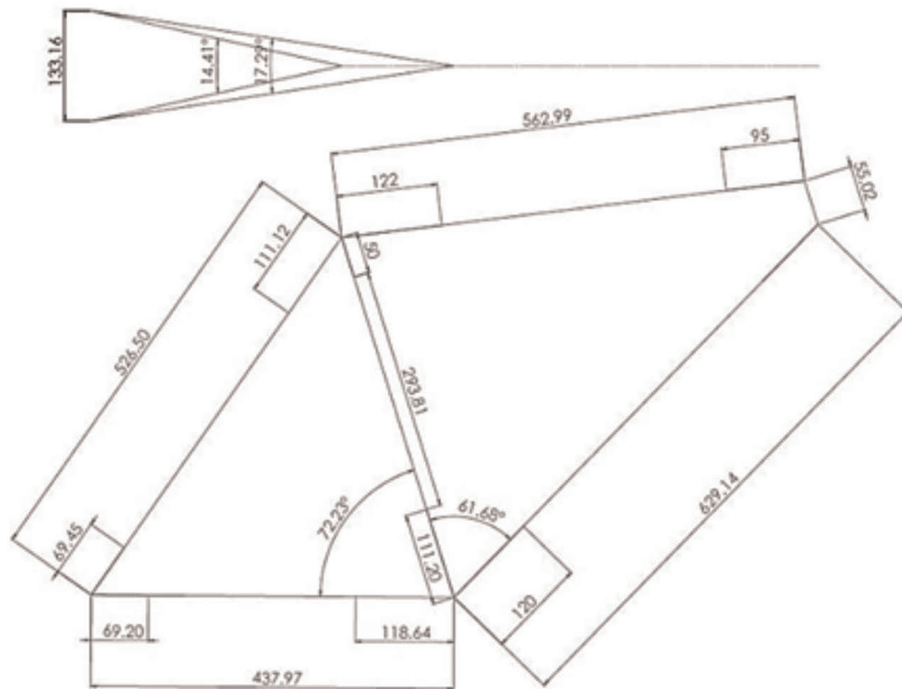
Figure 1.
Steeps followed.

supported beam according to ASTM D790-17 standards [16]; from this test Young's modulus was obtained. Bending tests were performed using a universal test machine UTS 200.3. Wood blocks were placed on load application points in order to avoid the load concentration effects (**Figure 4**).

Sixteen bamboo specimens with two sets of radii were tested, eight samples with 15.5 mm of outer radius and 10.5 of inner radius and another eight samples with
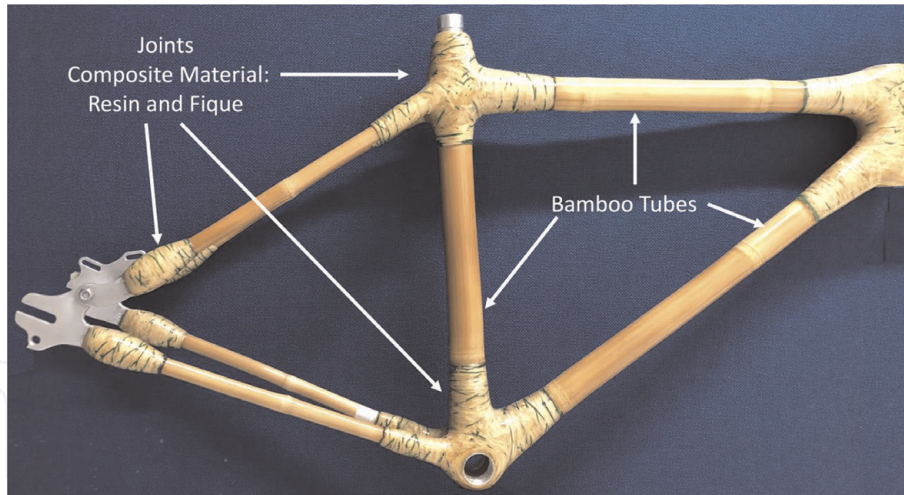
Figure 2.
Bamboo bike-frame.

Figure 3.
Bamboo bike-frame dimensions (in mm).

10.5 mm of outer radius and 10.25 mm of inner radius, approximately. A monotonically increasing load was applied to bamboo specimens until fracture and load versus displacement curves were obtained. The Young's modulus was calculated as explained below.

The *Y* displacement of the midspan of the specimen is:

$$Y = \frac{PL^3}{48EI} \tag{1}$$

Knowing the applied load (*P*) and the displacement (*Y*), the Young's modulus (E) must be obtained as:

$$E = \frac{PL^3}{48YI} \tag{2}$$

Figure 4.
Setup of three-point bending test.

where L is the distance between supports and I the inertia of the cross section. The inertia can be calculated as:

$$I = \frac{\pi}{64}\left(D_{outer}^4 - D_{inner}^4\right) \tag{3}$$

where D_{outer} is the outer diameter and D_{inner} is the inner diameter.
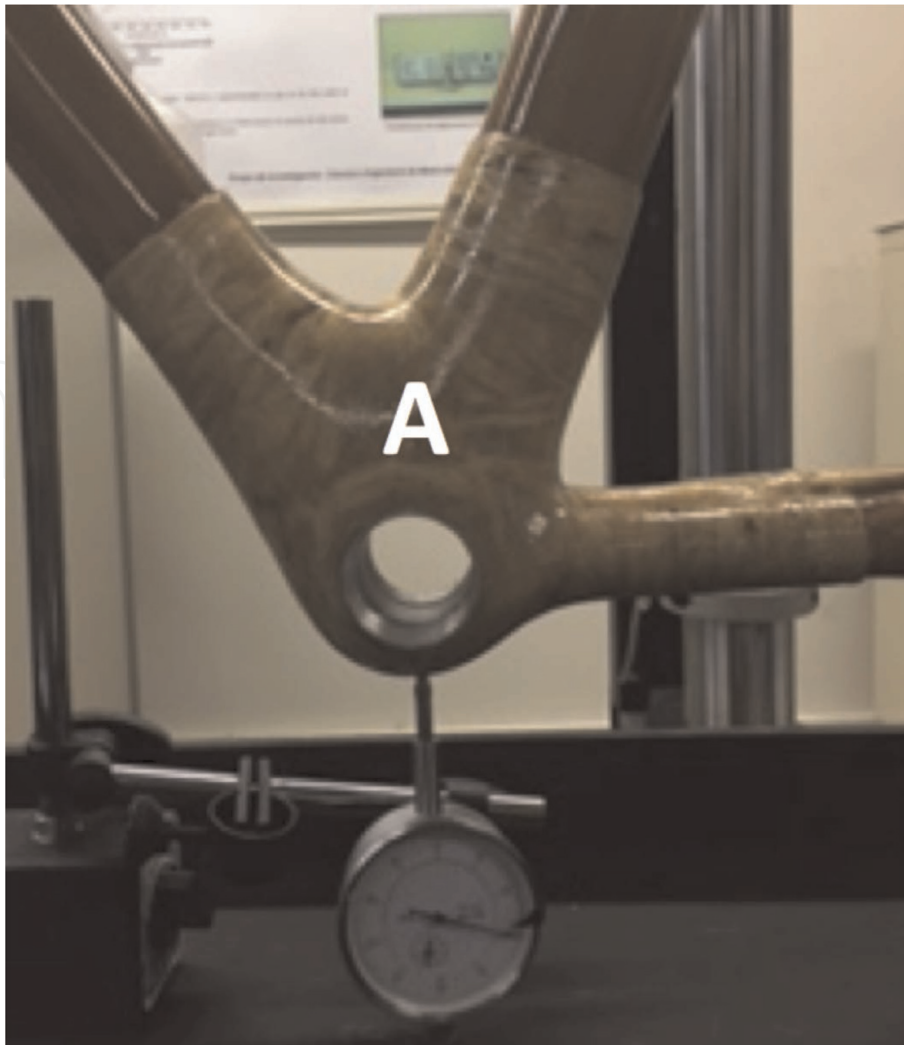
2.2.2 Experimental displacements

A universal test machine UTS 200.3 was used to obtain the experimental displacements of the A, B, and C points (**Figures 5** and **6**). Three load ramps were applied (2000, 3500, and 6500 N) on the seat tube (**Figure 7**) of the bike frame, and the displacements were measured. The experimental displacements of the bike frame were used to calibrate the numerical model.

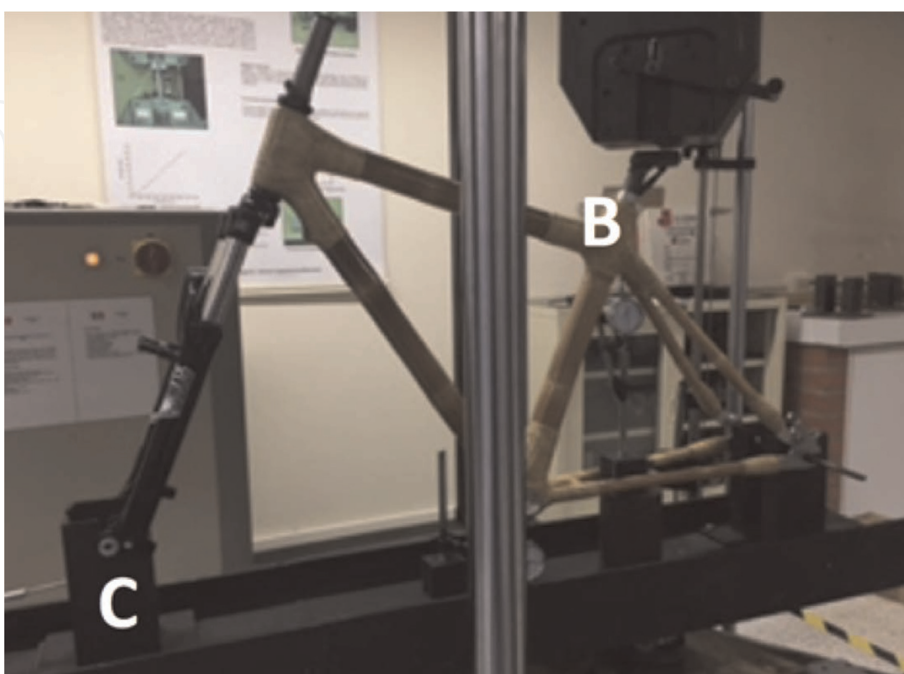### 2.2.3 Experimental natural frequencies

To validate the finite analysis model of the bike, experimental modal analysis of the frame was performed to obtain their natural frequencies and compare it to the results of the finite element model.

The experimental frequencies were obtained via a mobile application VibSensor [17], loaded on cell phones. The software provides the natural frequency on the system and its direction as responses to impulse loads are induced on the frame by tapping the frame several times at different locations with different intensities. The planes were defined by the phone (Z direction is normal to the screen of the phone).

In order to prove the accuracy of the mobile application, a simple model was used. The simple model consisted of a steel plate. The plate was fixed on both ends and the cell phone placed on the mid-length; then a load was applied to excite the plate, and their experimental natural frequencies were obtained. The first experimental natural frequencies were 19 Hz (**Figure 8**) and 19.95 Hz from the finite element model (**Figure 9**). In this direction, the accuracy of the mobile application was near to 5%. For this reason, the results obtained from the mobile application can be considered acceptable, and it can be used to the bamboo bike frame.
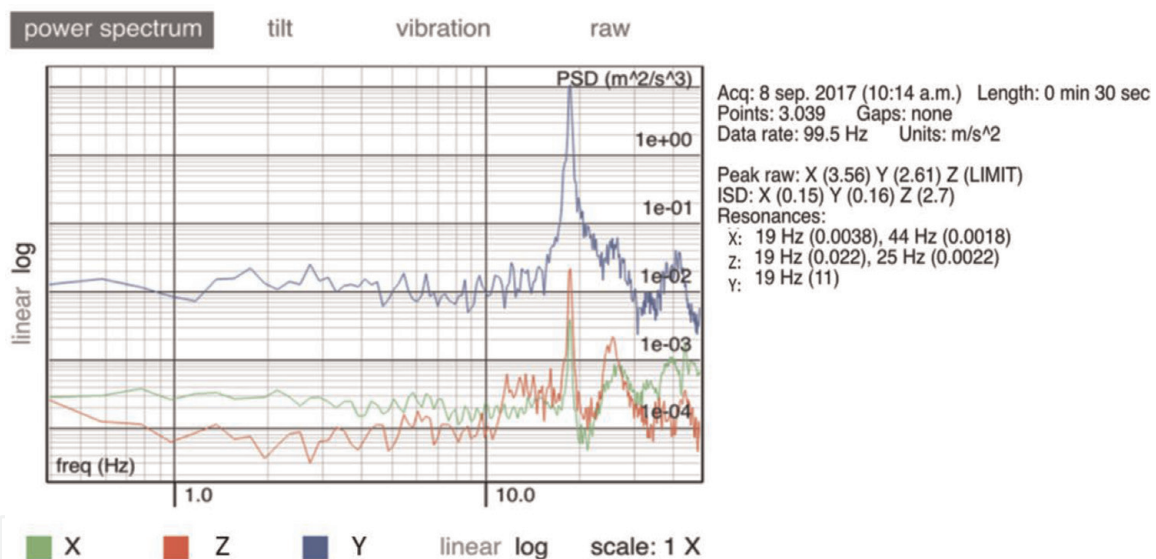
Figure 5.
Setup to measure the vertical displacement in bottom bracket joint, point A.

Figure 6.
Setup to measure the vertical displacement, points B and C.
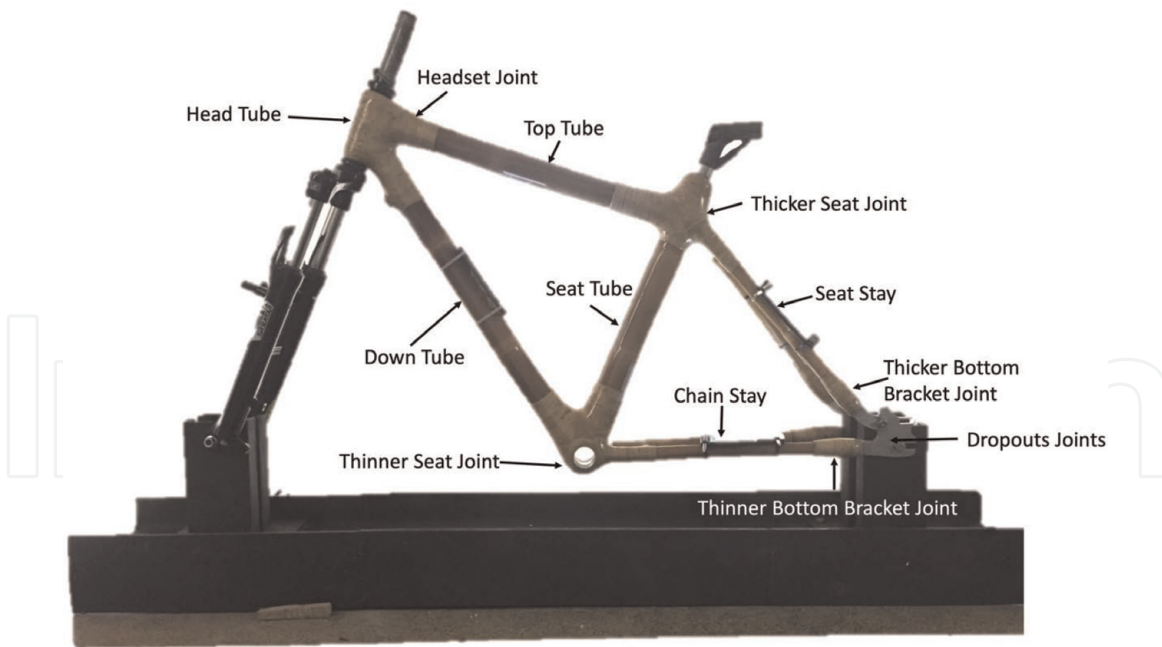
Figure 7.
Names of parts and joints of the bike.

Figure 8.
Experimental natural frequencies of the plate using Vibsensor software.

A setup was designed to obtain the natural frequencies of the bamboo bike frame (**Figure 10**). Cell phones were placed on three tubes: seat stay, chain stay, and down tube.

The bike frame was supported simulating the real conditions: the rear dropouts were fixed along x- and y-axes, and the front dropouts were fixed along y-axis and free along x-axis. The bike frame was excited using a load, and the cell phones registered the accelerations from which modal frequencies were processed, via a mobile application VibSensor.

2.3 Finite element model

The finite element analysis was performed using Abaqus 6.14-3 [18]. A static load of 3500 N and a moment of 350,000 N-mm were applied to the frame at the
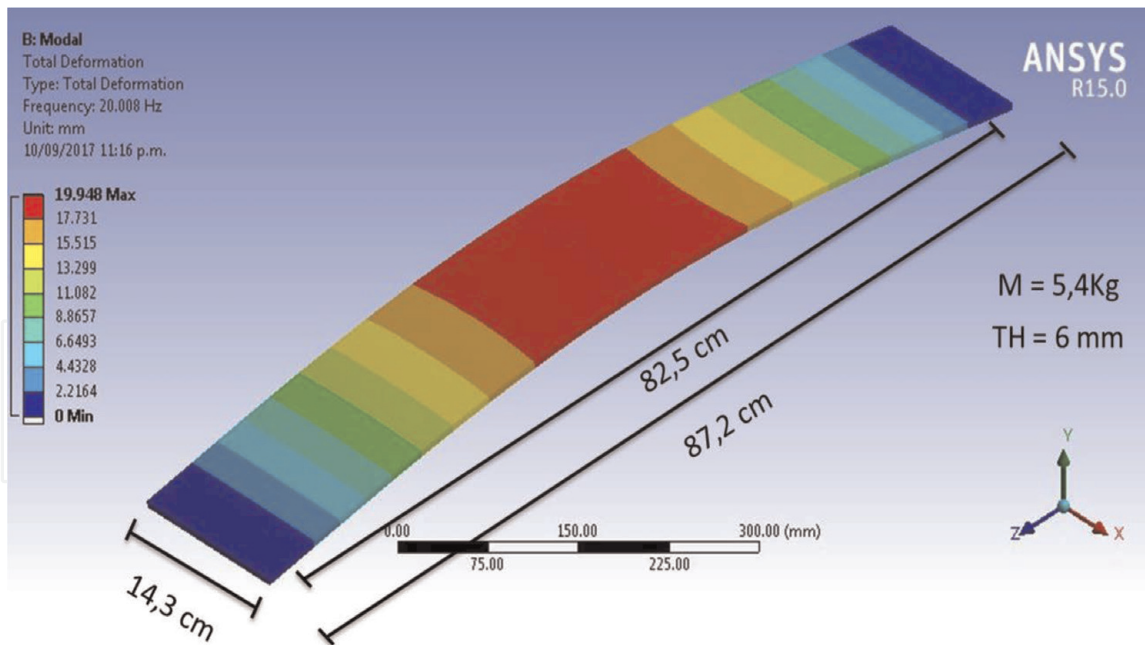
Figure 9.
*Natural frequencies of the plate using finite element model.*

Figure 10.
Setup of modal test.

saddle. The boundary conditions were defined as the rear dropouts were fixed along x- and y-axes, and the front dropouts were fixed along y-axis and free along x-axis (**Figure 11**). The elastic modulus was taken from the three-point bending tests.

The geometry was represented using straight bars and beam elements. A standard mesh was used in the model with an approximate global size of 60 mm per element. The cross section of each beam elements is shown in **Table 1**.

2.3.1 Model calibration

A SimFlow was created using iSight [19] and Abaqus software [18] in order to fit the displacement of the finite element model (A, B, and C points) with experimental values. The elastic module of the joints was considered as input, and the displacements of points A, B, and C were considered as output data.
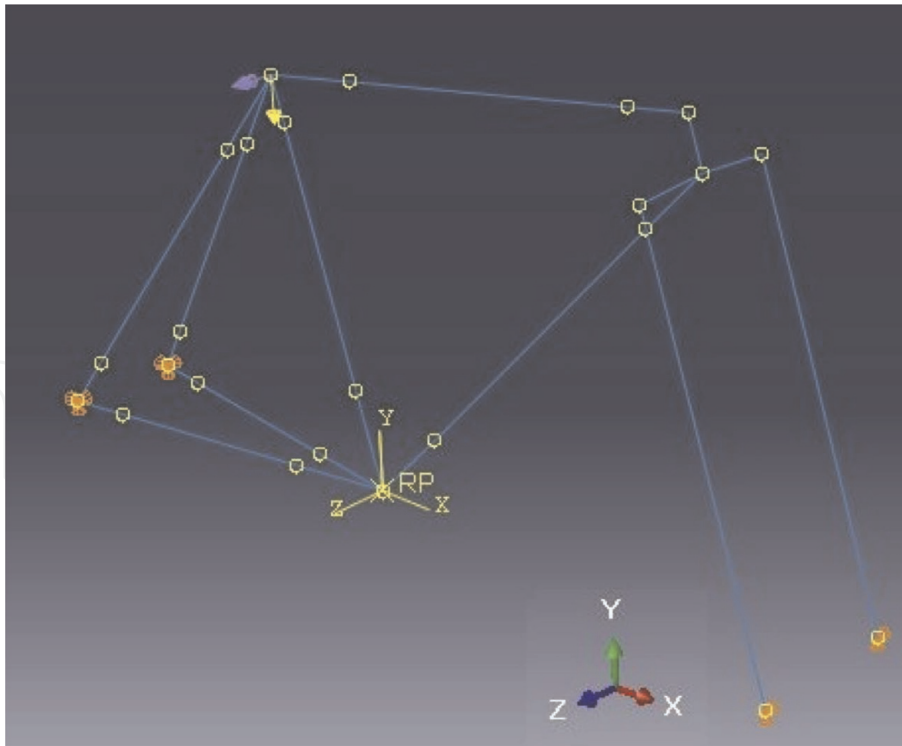
Figure 11.
Bike-frame finite element model.

Name part	Outer radius (mm)	Thickness (mm)
Down tube	15.5	5.o
Top tube	15.5	5.0
Seat tube	15.5	5.0
Seat stay	10.25	3.5
Chain stay	10.25	3.5
Thicker seat joint	25.0	10.5
Thinner seat joint	13.0	3.25
Headset joint	23.0	7.5
Thicker bottom bracket joint	25.0	10.5
Thinner bottom bracket joint	12.2	1.95
Dropouts joints	10.5	0.25

Table 1.
Cross sectional of the bike frame parts.

2.3.2 Model validation

The finite element model was validated comparing the experimental natural frequencies obtained in the 2.2.3 item with the modal analysis performed using Workbench/Ansys 19.0 software [20].

2.3.3 Fatigue analysis

Due to the bicycle moving on the irregular road, this induces loads dependent on the time on the bike frame. The fatigue strength is generally represented using alternative stress versus the number of cycles diagram, called the S-N curve.

The structural performance of the bike is important to corroborate the quality of products and to assign warranties. Some standards were found as ASTM F2711-08 [21], F2043-13 [22] and EN 14766 [23]. The standards to evaluate the fatigue performance of bicycle frames require a test setup where the frame is positioned at its normal attitude with the rear dropouts is free to rotate but without translation, while the front axle is free to translate and rotate. In this way, the whole frame is free to bend as it is the case when used on a road.

Fatigue analysis was performed using Workbench/Ansys software [20]. A bar is used to simulate the seat-stem, and it is inserted at 70 mm of distance from the top of the seat tube. The load at the bar simulates the weight of the rider (**Figure 11**). Then 50,000 test cycles load between 0 and 1200 N are applied vertically downward using a 25 Hz of frequency. From a practical standpoint, this cyclic load regime seems arbitrary and not related to any particular road the bicycle may be traveling.

Due to the impossibility of performing experiments to obtain the S-N curve of the bamboo, the S-N curve reported by Song et al. [24] was used to perform the finite element analysis.

Applying the Palmgren-Miner's [25] ratio to the bamboo bike frame, it was possible to determine their life in years:

$$Damage = \left(\frac{N_{applied}}{N_{allowed}} \right) \tag{4}$$

where $N_{applied}$ is obtained from the dynamic simulation obtained from the finite element analysis of the bicycle traveling a given distance, at a given speed, over a road of given characteristics, whereas $N_{allowed}$ is defined by the S-N curve. Where $N_{applied}$ is in cycles per kilometer.

2.3.4 Dynamic analysis

A dynamic analysis of the bike frame was performed. A displacement vs. time function was applied (**Figure 12**) at the front and rear dropout nodes and spring elements used to simulate the tires and fork stiffness (**Figure 13**).

The displacement prescription was obtained from the technical specification of the speed reducer, 6 cm of height and 37 cm of width (**Figure 12**); also we used a bicycle speed of 25 km/h.

Using the road profile and knowing that the wavelength $\lambda = 0.74\ m$, the frequency $f = 9.57\ Hz$ and the angular velocity $\omega = 9.57\ Hz$; the movement equation is:

$$y = 0.06 \sin 58.92t \tag{5}$$

The spring constant (**Figure 13**) was calculated using the vertical deflection of the tire of the bicycle measured at the laboratory under applying a weight. As results were obtained, K = 15.5 N/mm for the rear tire and K = 56.93 N/mm for the front tire. The model was restricted to all translation degrees on dropouts and fixed the displacement in the *Z*-axis on the fork.

Figure 12.
Road profile (distances in mm).
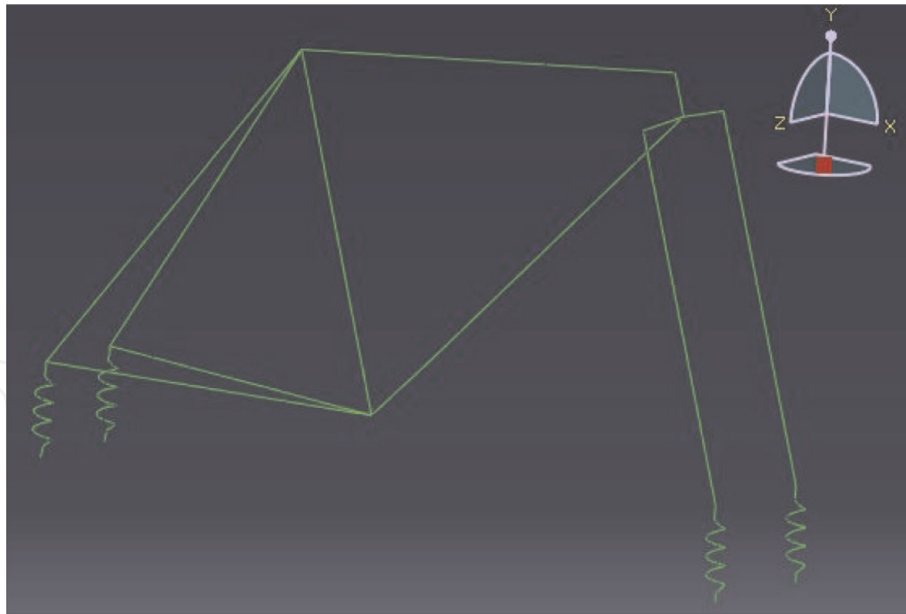
Figure 13.
*Finite element model of the bike.*

3. Results

3.1 Three-point bending tests

The Young's module was calculated using Eq. (2), and the displacements obtained from three-point bending tests (**Figure 14**). The average values were 9420.8 MPa for the large diameter bamboo and 12610.3 MPa for the small diameter (**Table 2**).

Additionally, the coefficient of variation for a thicker bamboo was good (4.9) considering the variability of the bamboo as a biological material; instead, for thinner bamboo, the variability was 2.7 times higher (**Table 2**).

3.2 Experimental displacements

The maximum displacements were obtained on C point followed by B point and A point (**Table 3**). The behavior of the displacement versus load was lineal, to all points.
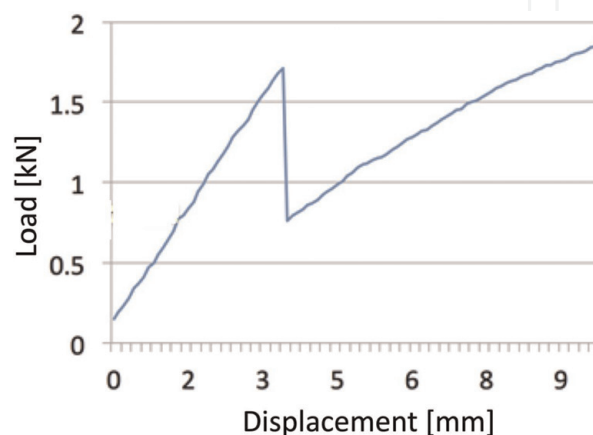
Figure 14.
Typical load vs. displacement curve of bamboo specimen, three-point bending test.

	Thicker bamboo	Thinner bamboo
Average [MPa]	9420.8	12610.3
Standard deviation [MPa]	459.4	1668.9
Coefficient of variation (%)	4.9	13.3
Minimum [MPa]	8589.3	10015.0
Maximum [MPa]	10551.2	14764.8

Table 2.
Longitudinal Young's module for bamboo.

Load	Points displacement (mm)		
	A	B	C
2000 N	−0.06	−2.19	5.09
3500 N	−2.89	−4.14	9.36
6000 N	−5.17	−7.43	16.34

Table 3.
Average of vertical (A and B) and horizontal (C) displacements.

3.3 Finite element model

3.3.1 Model calibration

To calibrate the finite element model, a load of 3500 N and a moment of 35,000 N-mm were used. The target of the model was to fit the displacement of A point near to the experimental displacement, −2.89 mm along *y*-direction (**Table 3**). The range of Young's modulus used to the joints was 6000–200,000 MPa. The solution converged for a range of Young's modulus between 6000 and 9880 MPa (**Table 4**).

3.3.2 Model validation

Young's modulus obtained from the calibration process (**Table 4**) was used to define the rigidity of the joints. The model was validated using the experimental natural frequency (**Figure 15**), and the first modal shape of the bike frame was out of the plane (*Z*) with a natural frequency of 38.0 Hz (**Figure 15**). For the finite element model, the first natural frequency was 35.0 Hz (**Figure 16**). The difference between the experimental result and the finite element model was 7.9%.
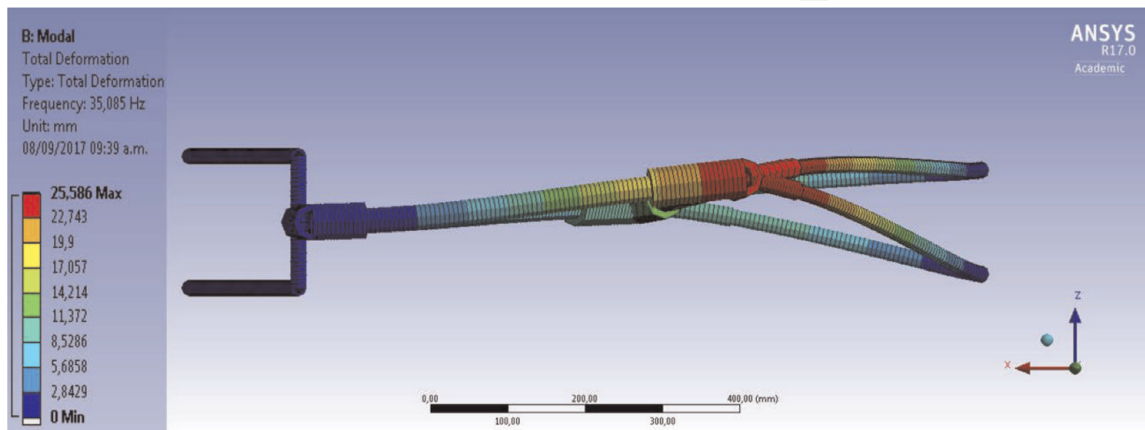
This difference may be due to the difficulty of exactly modeling the supports and material properties, specifically at the fork and the joints. These results show

Zone	E (MPa)
Bottom bracket	8061
Dropouts joint	6000
Headset	9880
Seat joint	6000

Table 4.
Young's modulus from model calibration.
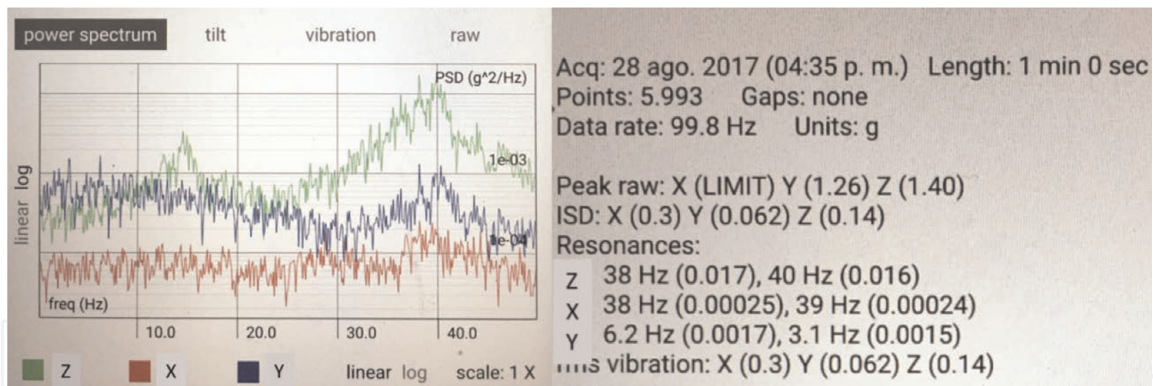
Figure 15.
*Experimental first modal mode.*

Figure 16.
*First modal mode using finite element analysis modal.*

that the model represents satisfactorily the real bike frame. Then, these results can be used to fatigue analysis using the finite element method.

3.4 Dynamic response of the finite element model

Using the finite element model calibrated and validated, a dynamic response analysis was performed. The maximum reaction force at dropout joint zone was 114 N (**Figure 17**), the maximum stress was 114.6 MPa at the dropout, and the maximum displacement was 70.6 mm at the seat joint (**Figure 18**, **Table 5**). The
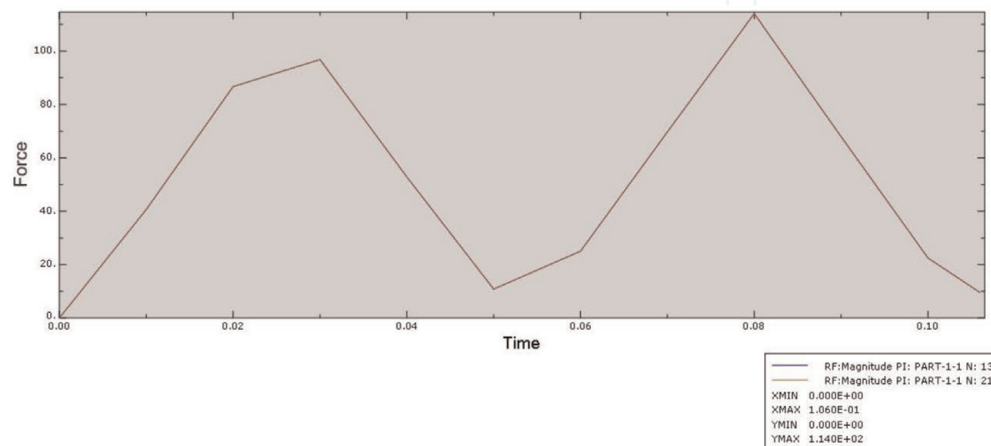
Figure 17.
Reaction force profile at dropout joint zone.
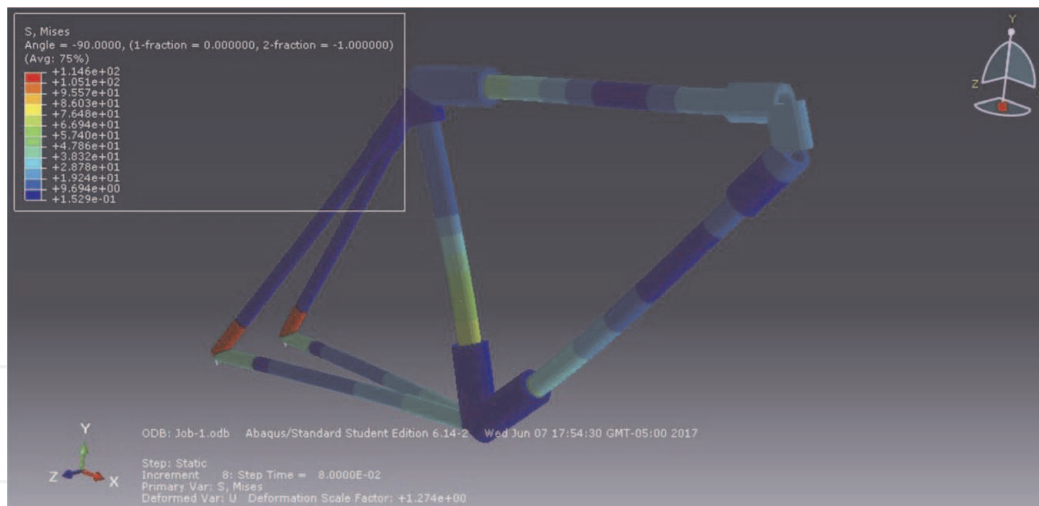
Figure 18.
Results of dynamical analysis simulation.

Control points	Maximum stress (MPa)	Maximum displacement (mm)
Seat joint	15.6	70.6
Bottom bracket	34.3	59.8
Fork	19.6	34.0
Dropout	114.6	0.0

Table 5.
Maximum stress and displacements at control points.

results show that the maximum stress occurs at dropout joints; hereby, this joint requires special attention.

From on the dynamic simulation of bike frame and assuming that the bike travel at 25 km/h, with a rider of 100 kg, and a road with contiguous bumps of 6 cm in height and 34 cm in length. The mechanical response at the intersection between the seat stay and the rear dropout was 114 MPa. Using a rate of application of 1351 cycles/km, 90 km is the distance a rider rides per week. Then, for a year the distance is 4680 km, and assuming a life of the bike of 10 years, the bike works:

$$N_{applied} = \left(4680 \, \frac{kilometer}{year} \right) \times (10 \, years) \times \left(1351 \, \frac{N}{kilometer} \right) \qquad (6)$$

$$N_{applied} = 6.3 \times 10^7 \, cycles \qquad (7)$$

Using the bamboo fatigue S-N curve reported by Song [24] and the stress profile obtained from the dynamic analysis (**Figure 19**), a fatigue analysis was performed. The life obtained was 1.7×10^9 cycles, the damage ratio, $N_{applied}/N_{allowed} = 0.037$; this indicates that the bike frame would last 26 times longer than its intended use; then the fatigue life of the frame will be more than 100 years, for these work conditions.

4. Discussion and conclusions

The relatively large scatter obtained for the elastic moduli can be explained by the non-exactly replicated nature of the bamboo material from plant to plant [25]. The differences of Young's moduli between thicker and thinner diameter bamboo
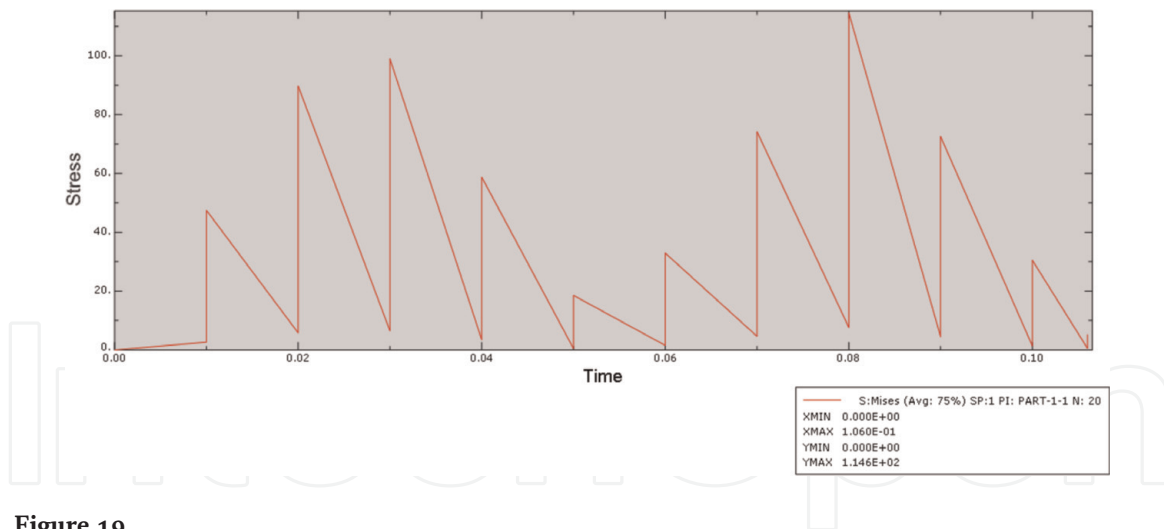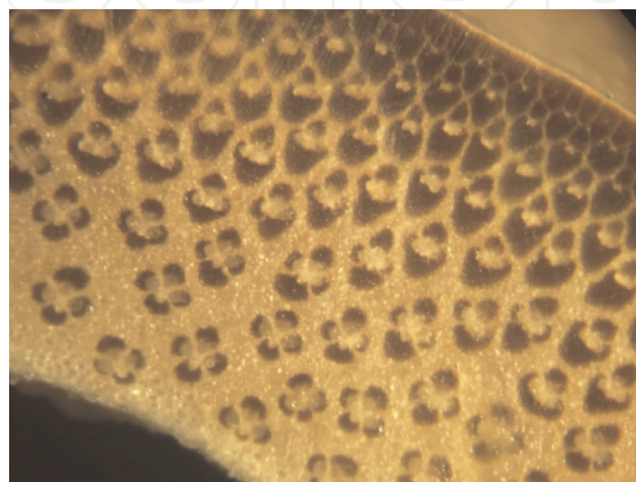
Figure 19.
Stress vs. time profile from dynamical response of the frame.

specimens may be explained by the differences between the compaction of the bamboo structure or the relation between the thickness and diameter of the bamboo samples, depending on the zone of the stem where the specimens were extracted.

In general, bamboo is thicker at the top than at the base of the culms [25]. Comparing the structures for the different diameters, the thinner diameter bamboo (**Figure 20**) has a structure more compact than the thicker diameter bamboo (**Figure 21**) and consequently higher Young's modulus [26].

The vascular bundle is a small longitudinal interstice of the bamboo stem (**Figures 20** and **21**). It affects directly the mechanical properties of the specimen due to these pores that act as stress concentrations. Kanzawa et al. [27] proposed to measure the maximum width and length of the vascular bundles (**Figure 22**). In this work, an average of 0.45 mm length and 0.38 mm width for thicker bamboo and 0.19 mm length and 0.14 mm width for thinner bamboo. Because the gap in the thinner bamboo is smaller than the thicker bamboo, the Young's modulus in the thinner is going to be higher making it more rigid.

In addition, a dynamic simulation of the bamboo frame was performed to obtain the acting forces at the bike frame and thus the stresses, at the most critical joint entering the rear dropout. With this information, the generic specimen representative of this joint was prepared to generate additional fatigue data to evaluate the useful life of the frame in future works (**Figure 23**).
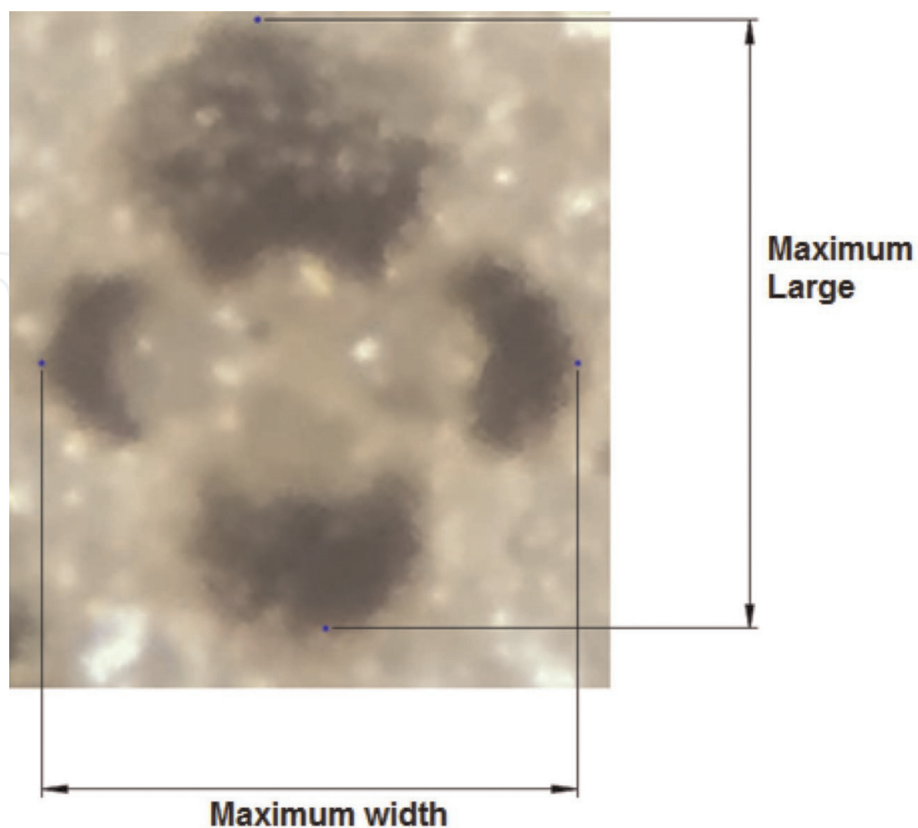

Figure 20.
Microscopical section view for thinner bamboo specimen (1×).
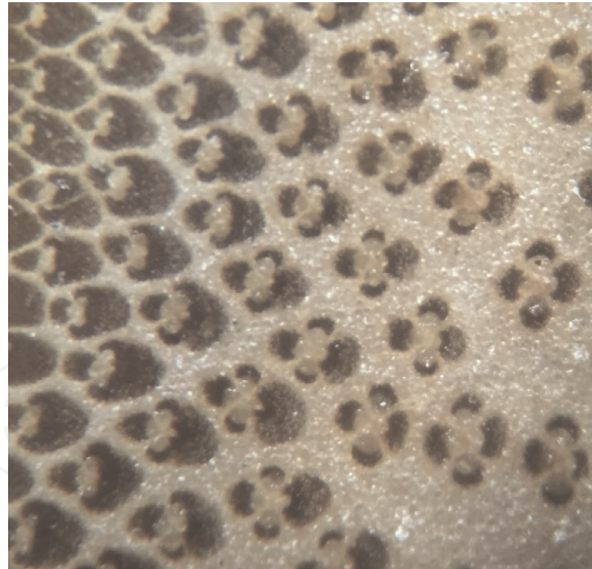
Figure 21.
Microscopical section view for thicker bamboo specimen (1×).

Finally, a methodology was proposed to evaluate the fatigue life of the bamboo bike frame from the experimental data reported for bamboo samples. However, the results should be taken as an approximation because the fatigue life of the bamboo bike frame has a high dependency on their joints. In this direction and in future works, it is necessary to perform fatigue experiments using the whole bike frame or at least to test the joints separated. This can be explained as there are substantial differences between the fatigue life of base material and the fatigue life of the final product. Also, some technical values of bamboo bike frames were obtained, so that

Figure 22.
Vascular bundle scheme in a section view of a bamboo specimen.

Figure 23.
Generic specimen representative of the rear dropout joint.

these will allow them to define the technical characteristics of the product and guarantee their operating conditions.

Acknowledgements

Conflict of interest

The author declares that there is no conflict of interest regarding the publication of this chapter.

Author details

Juan P. Arango Fierro[1], Jose L. Arango Fierro[1] and Héctor E. Jaramillo Suárez[2*]

1 Mechanical Engineering Program, Autónoma de Occidente University (UAO), Cali, Colombia

2 Energetic and Mechanical Department, Autónoma de Occidente University (UAO), Cali, Colombia

*Address all correspondence to: hjsuarez@uao.edu.co

IntechOpen

References

[1] Tai S-YTT, Veraart F, Davids M. How the Netherlands became a bicycle nation: Users, firms and intermediaries, 1860–1940. Business History. 2015;**57**: 257-289. DOI: 10.1080/00076791. 2014.928695

[2] Peterson LA, Londry KJ. Finite Element Structural Analysis: A New Tool for Bicycle Frame Design, (n.d.). https://www.sheldonbrown.com/rinard/fea.htm [Accessed: April 26, 2019]

[3] Cicero S, Lacalle R, Cicero R, Fernández D, Méndez D. Analysis of the cracking causes in an aluminium alloy bike frame. Engineering Failure Analysis. 2011;**18**:36-46. DOI: 10.1016/j. engfailanal.2010.08.001

[4] Liu TJ-C, Wu H-C. Fiber direction and stacking sequence design for bicycle frame made of carbon/epoxy composite laminate. Materials & Design. 2010;**31**: 1971-1980. DOI: 10.1016/j. matdes.2009.10.036

[5] Lessard LB, Nemes JA, Lizotte PL. Utilization of FEA in the design of composite bicycle frames. Composites. 1995;**26**:72-74. DOI: 10.1016/0010-4361 (94)P3633-C

[6] Alves ME, Pereira TVC, Gomes O, Silva F, Toledo RD. The effect of fiber morphology on the tensile strength of natural fibers. Journal of Materials Research and Technology. 2013;**2**: 149-157. DOI: 10.1016/j. jmrt.2013.02.003

[7] Zakikhani P, Zahari R, Sultan MTH, Majid DL. Extraction and preparation of bamboo fibre-reinforced composites. Materials & Design. 2014;**63**:820-828. DOI: 10.1016/j.matdes.2014.06.058

[8] Osorio L, Trujillo E, Van Vuure AW, Verpoest I. Morphological aspects and mechanical properties of single bamboo fibers and flexural characterization of bamboo/epoxy composites. Journal of Reinforced Plastics and Composites. 2011;**30**:396-408. DOI: 10.1177/ 0731684410397683

[9] Ben-Zhi Z, Mao-Yi F, Jin-Zhong X, Xiao-Sheng Y, Zheng-Cai L. Ecological functions of bamboo forest: Research and application. Journal of Forestry Research. 2005;**16**:143-147. DOI: 10.1007/BF02857909

[10] BambooCo Bikes Project. EcoCultura. n.d. Available at: https:// ecoculturablog.wordpress.com/about-bambooco-bikes/ [Accessed: April 26, 2019]

[11] Porque el diseño tiene sentido—talleres ambientales. Corporación Laboratorio de Diseño Sostenible, Coladisos—talleres de sensibilización ambiental, (n.d.). Available at: https:// coladisos.jimdo.com/ [Accessed: April 26, 2019]

[12] Calfee Design–Bicycles and Components, Carbon Repair, DIY Bamboo Kits. n.d. https://calfeedesign. com/ [Accessed: April 26, 2019]

[13] Kingsley U, Imoisili PE, Adgidzi D. Finite element analysis of bamboo bicycle frame. British Journal of Mathematics & Computer Science. 2014;5:583-594

[14] Covill D, Begg S, Elton E, Milne M, Morris R, Katz T. Parametric finite element analysis of bicycle frame geometries. Procedia Engineering. 2014; **72**:441-446. DOI: 10.1016/j. proeng.2014.06.077

[15] Cheng Y-C, Lee C-K, Tsai M-T. Multi-objective optimization of an on-road bicycle frame by uniform design and compromise programming. Advances in Mechanical Engineering. 2016;**8**. DOI: 10.1177/1687814016632985

[16] ASTM D790-17. Standard Test Methods for Flexural Properties of Unreinforced and Reinforced Plastics and Electrical Insulating Materials. ASTM International. 2017

[17] VibSensor 2.1.1 Free Download. n.d. Available at: https://vibsensor.soft112. com/ [Accessed: April 30, 2019]

[18] SIMULIA. Software de simulación 3D-Dassault Systèmes®. n.d. https:// www.3ds.com/es/productos-y-servic ios/simulia/ [Accessed: April 30, 2019]

[19] Isight y SIMULIA™ Execution Engine - Dassault Systèmes®. n.d. https://www.3ds.com/es/productos-y-se rvicios/simulia/productos/isight- y-simulia-execution-engine/ [Accessed: April 30, 2019]

[20] Engineering Simulation & 3D Design Software. ANSYS. (n.d.). Available at: https://www.ansys.com/ [Accessed: April 30, 2019]

[21] ASTM F2711-08. Standard Test Methods for Bicycle Frames. ASTM International. 2012

[22] ASTM F2043-13. Standard Classification for Bicycle Usage. ASTM International. 2015

[23] UNE-EN 14766. Mountain-bicycles—Safety requirements and test methods. Asociación Española de Normalización. 2006

[24] Song J, Utama J, Hu D, Lu Y. Fatigue characterization of structural bamboo materials under flexural bending. International Journal of Fatigue. 2017;**100**:126-135. DOI: 10.1016/j.ijfatigue.2017.03.016

[25] Zhang Y, Yu W. Effects of thermal treatment on surface color, dimensional stability and mechanical properties of bamboo-based fiber composites. In: Proceedings of 2012 International Conference on Biobase Material Science and Engineering. 2012. pp. 132-136. DOI: 10.1109/BMSE.2012.6466197

[26] Habibi MK, Lu Y. Crack propagation in bamboo's hierarchical cellular structure. Scientific Reports. 2014;**4**:5598. DOI: 10.1038/srep05598

[27] Kanzawa E, Aoyagi S, Nakano T. Vascular bundle shape in cross-section and relaxation properties of Moso bamboo (*Phyllostachys pubescens*). Materials Science and Engineering: C. 2011;**31**:1050-1054. DOI: 10.1016/j. msec.2011.03.004